

## Terahertz transmission of a $\text{Ba}_{1-x}\text{K}_x\text{BiO}_3$ film probed by coherent time-domain spectroscopy

F. Gao,\* J. F. Whitaker, Y. Liu, and C. Uher†

*Center for Ultrafast Optical Science, University of Michigan, Ann Arbor, Michigan 48109*

C. E. Platt and M. V. Klein‡

*Science and Technology Center for Superconductivity, University of Illinois at Urbana-Champaign, Urbana, Illinois 61801*

(Received 14 July 1994; revised manuscript received 29 December 1994)

The complex transmission coefficient for millimeter and submillimeter waves incident on a  $\text{Ba}_{0.6}\text{K}_{0.4}\text{BiO}_3$  thin film (82 nm) has been measured over a frequency range of 200–1200 GHz at temperatures above and below  $T_c$  using coherent time-domain spectroscopy. We observe a dramatic change in both the magnitude and phase of the terahertz transmission in the superconducting state caused by a rapid carrier condensation. Both the real ( $\sigma_1$ ) and imaginary ( $\sigma_2$ ) parts of the complex conductivity are determined directly from the amplitude and phase of the transmitted electric field without the need for a Kramers-Krönig analysis. By fitting  $\sigma_2$  in the framework of BCS theory, a superconducting gap  $2\Delta(0) = 6.9 \text{ meV} = 3.8k_B T_c$  is obtained. Below  $T_c$ , the  $\sigma_1$  is rapidly enhanced for  $\omega/2\pi < 500 \text{ GHz}$ , which is attributed to the BCS coherence effects. However, the conductivity exhibits monotonic temperature dependence and no clear  $\sigma_1(T)$  peak is observed throughout the frequency range measured. The high-frequency penetration depth ( $\sim 600 \text{ nm}$ ) is also extracted and discussed. Our results are consistent with a picture of BCS moderate coupling superconductivity in an intermediate to dirty limit.

### I. INTRODUCTION

The  $\text{Ba}_{1-x}\text{K}_x\text{BiO}_3$  (BKBO) compound is a copper-free cubic oxide which is of interest as an intermediate-temperature superconductor. It is attractive for potential device applications because it has a lower microwave loss than copper,<sup>1,2</sup> an isotropic structure, and a moderately long coherence length ( $\sim 60 \text{ \AA}$ ). These properties provide BKBO with some advantages in applications compared to high- $T_c$  cuprates that have a highly anisotropic structure and an extremely short coherence length ( $\sim 3 \text{ \AA}$ ). The superconducting transition temperature of BKBO ( $\sim 30 \text{ K}$  in bulk forms) is, although not high compared with cuprates, higher than all conventional low- $T_c$  superconductors (LTS's), despite its low density of states near the Fermi energy in the normal state.<sup>3</sup> Technologically, this material has exhibited excellent BCS-like quasiparticle tunneling characteristics in BKBO/Au junctions<sup>4,5</sup> and hysteretic Josephson tunneling behavior in BKBO/BKBO contacts.<sup>6–8</sup> Such results are difficult to observe in copper-oxide-based high- $T_c$  superconductors (HTS's) because of their extremely short coherence lengths and two-dimensional characteristics. From a scientific perspective, the BKBO exhibits many BCS-like and HTS-like characteristics, and for this reason it is frequently stated that this material bridges the gap between the conventional and high-temperature superconductors.

The high-frequency properties of superconductors are important for their intrinsic nature as well as for device applications. Measurements of the temperature and frequency dependence of the complex conductivity ( $\sigma = \sigma_1 + i\sigma_2$ ) provide a powerful probe of electron dynamics. The  $\sigma_1$  characterizes the excitation of unpaired quasiparticles by absorption of photons of energy  $\hbar\omega$ , while the  $\sigma_2$  describes the nondissipative supercurrent

and the condensation of the superconducting electrons. Other important parameters such as the surface impedance, magnetic penetration depth, superfluid density, superconducting energy gap, and quasiparticle scattering time can also be extracted from  $\sigma$ .

BKBO may follow the conventional BCS pairing mechanism as evidenced by a BCS-like isotope effect,<sup>3</sup> a BCS-like tunneling gap,<sup>3,7–9</sup> and an *s*-wave-like (exponential temperature dependence) microwave penetration depth.<sup>10</sup> Early infrared reflectance measurements have also showed features identified as a weak-coupling superconducting gap of  $2\Delta/k_B T_c = 3.5 \pm 0.5$ .<sup>11</sup> On the other hand, these bismuthates share many similar properties with cuprates and have their own unusual characteristics that are not yet well understood. However, in contrast to high- $T_c$  cuprates such as  $\text{YBa}_2\text{Cu}_3\text{O}_7$  (YBCO), BKBO has received considerably less research attention, particularly in optical studies. Recently, a number of groups have investigated this material in hope of elucidating its doping<sup>12,13</sup> and temperature<sup>14</sup> dependencies using optical power reflectance measurements. Others have aimed to determine the penetration depth of BKBO through microwave surface-resistance measurements.<sup>10</sup> These studies were made either over a frequency range above the superconducting gap [50–10 000  $\text{cm}^{-1}$ , i.e., 1.5–300 THz (Refs. 12–14)] or with regard to a single frequency (6 GHz) much below the gap energy.<sup>10</sup> Most recently, Dunmore *et al.*<sup>15</sup> observed a pronounced BCS-like peak near 50  $\text{cm}^{-1}$  (1.5 THz) in the power transmittance for two BKBO films ( $T_c = 18$  and 14 K) and suggested that the materials were in the strong-coupling dirty limit. One well-known drawback in determining the low-frequency conductivities using power reflectance or transmittance spectroscopy involves the use of a Kramers-Krönig analysis.<sup>16</sup> Measurements over a

sufficiently large frequency range—which are not feasible for transmittance due to substrate effects—and an artificial extrapolation to zero frequency are then required. In addition, the accuracy at low frequencies suffers significantly, especially when the reflectance is close to unity,<sup>17–19</sup> as is the case in the superconducting state. As alternatives, one can obtain the frequency-dependent conductivities of thin films without the need for the Kramers-Krönig transform by measuring, in any finite frequency range of interest, *both* the power transmittance *and* reflectance<sup>20,21</sup> or *both* the amplitude *and* phase of the transmitted field.<sup>22</sup>

In this paper we present complex terahertz field-transmission (amplitude and phase) data for a BKBO film above and below  $T_c$  using a coherent time-domain spectroscopy technique. As a bridge between the microwave and infrared spectra previously studied, our millimeter- and submillimeter-wave spectra cover a range (0.2–1.2 THz) which until now has not been investigated. This range is near and below the superconducting gap frequency, thus providing a picture of the low-energy excitations and the superconducting dynamics in this material. Our results, including a superconducting gap inferred from  $\sigma_2$  and the absorption observed in  $\sigma_1$  below the gap, are consistent with existing infrared and microwave studies<sup>10,11,14,15</sup> and support the BCS model for bismuthate materials, in contrast to the high- $T_c$  cuprates.

## II. EXPERIMENT

The experimental setup of our terahertz spectrometer has been described earlier<sup>23</sup> and is similar to the one demonstrated by van Exter and Grischkowsky.<sup>24</sup> An ultrafast, self-mode-locked Ti:sapphire laser ( $\sim 100$ -fs duration pulses with 90-MHz repetition rate) is used as an optical source for exciting transmitter and receiver photoconductive antennas. These elements are Hertzian dipole antennas consisting of coplanar-strip transmission lines with  $20\text{-}\mu\text{m}$  width and separation fabricated on ultrashort-lifetime, low-temperature-grown GaAs wafers.<sup>25</sup> The transmitter, biased with a dc voltage and triggered by pump-laser pulses, emits a short electromagnetic burst with a broad dipole radiation spectrum. The radiation is directly incident on the unpatterned sample under study, and the transmitted signal is focused on the receiver. The latter element contains a photoconductive sampling gate with a temporal resolution that limits the system response to about 2 THz. The induced transient current from the receiver sampling gate is proportional to the electric field induced by the radiated transient on the receiving antenna. The photocurrent from the receiver corresponding to the radiated wave form in the time domain is obtained using probe (i.e., gating) laser pulses that are synchronized and variably delayed with respect to the pump, or excitation, pulses.

The  $\text{Ba}_{1-x}\text{K}_x\text{BiO}_3$  film was grown with a nominal doping of  $x=0.4$  on a  $0.54\text{-mm}$ -thick magnesium oxide (MgO) substrate by *in situ* pulsed laser deposition.<sup>26</sup> It was deposited from a  $\text{Ba}_{0.55}\text{K}_{0.45}\text{BiO}_3$  target made at Argonne National Laboratory<sup>27</sup> by a melt quench process. The substrate was attached to a resistive heater block

with silver paste, and the heater temperature was monitored by a thermocouple mounted inside the block. The chamber was pumped to  $10^{-6}$  Torr while the substrate was hot, then the film deposition was carried out at a block temperature of  $600^\circ\text{C}$  in pure argon at a pressure of 1 Torr and with a laser power of 260 mJ/pulse. The film growth rate was 70 nm/min. After deposition, the film was quickly cooled ( $35^\circ\text{C}/\text{min}$ ) to  $400^\circ\text{C}$  and oxygenated in a 10-min soak, then cooled to room temperature. The film thickness was  $82\pm 5$  nm measured by step profilometry, and the transition temperature was  $\sim 21$  K with  $\Delta T_c = 3$  K, determined by measuring the magnetic susceptibility using a superconducting-quantum-interference-device (SQUID) magnetometer. We note that MgO is ideal as a thin-film substrate for transmission studies because it is quite transparent<sup>20</sup> and virtually dispersionless and lossless<sup>28</sup> across the entire bandwidth of our terahertz radiation system in the temperature range presented here. The incident electric field was polarized parallel to the sample surface. The transmitter, the receiver, and the sample under study were housed inside a vacuum chamber. The sample was mounted to a cold finger and was cooled by continuous helium flow so that the temperature could be varied between 5 and 300 K. A blank substrate identical to the one supporting the thin film was used as a reference. By doing the fast Fourier transform (FFT) of the temporal response data, we obtained simultaneously both the field amplitude and the phase transmitted through the thin-film/substrate composite in the frequency domain. The experimental data usually exhibit a high signal-to-noise ratio; thus data smoothing is unnecessary for analysis.

When the film thickness,  $d$ , is much smaller than the

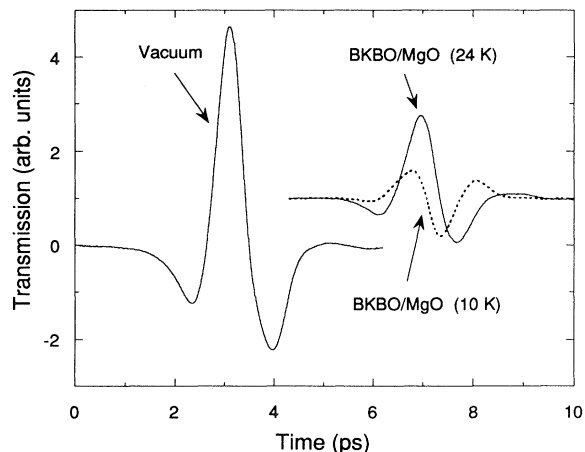


FIG. 1. Time-domain spectroscopy comparing transmission of ultrashort radiating pulses through vacuum and a BKBO film on MgO at selected temperatures just above and at about half of  $T_c$  ( $\sim 21$  K). A remarkable change in line shape is seen for  $T < T_c$ . The  $\sim 3.8$ -ps time delay with the sample in position is caused by the underlying  $0.54\text{-mm}$  MgO substrate. Note, for clarity, the curves for the BKBO/MgO have been shifted upward by one vertical unit.

penetration depth and the wavelength, as is the case here, the measured complex field-transmission coefficient,  $t$ , is related to the complex conductivity of the film,  $\sigma$ , by

$$t = \frac{E_{\text{film/substrate}}}{E_{\text{vacuum}}} = \frac{2}{N+1+Z_0 d \sigma} \frac{2N}{N+1} e^{i(N-1)(\omega/c)s}. \quad (1)$$

Here  $E_{\text{vacuum}}$  and  $E_{\text{film/substrate}}$  are the induced electric fields on the receiver after the terahertz beam passes through vacuum (blank hole) and the thin film on substrate, respectively.  $Z_0 = 377 \Omega$  is the impedance of free space, and  $N$  and  $s$  are the complex refractive index and thickness, respectively, of the underlying substrate. In this experiment,  $N = n + i\kappa$  was determined by measuring a blank MgO reference. It was found that  $n \approx 3.10 \pm 0.02$ , with only very little dispersion, and  $\kappa/n \ll 1\%$  throughout the frequency range measured. Note Eq. (1) neglects the multiple internal reflections inside the underlying substrate. For a 0.5-mm-thick MgO, the round-trip time would be  $\sim 10$  ps, which is much larger than the primary pulse width ( $\sim 2$  ps) as illustrated in Fig. 1. Thus we can easily separate out the internal reflections before doing the FFT. On the other hand, it should be pointed out that Eq. (1) takes into account multiple internal reflections from within the thin film.

### III. RESULTS AND DISCUSSION

Figure 1 demonstrates the time-domain spectra obtained for radiation through vacuum and with a BKBO-on-MgO sample between the antennas. The MgO substrate causes a time delay relative to vacuum by  $\Delta t = (n-1)s/c$ . Above  $T_c$ , the transmitted terahertz pulse is almost undispersed, as shown by the data taken at 24 K, and the reduction in the transmitted signal is primarily due to reflection from the film, as well to some metallic absorption. Upon entering the superconducting state, besides a further decrease in amplitude, there is a

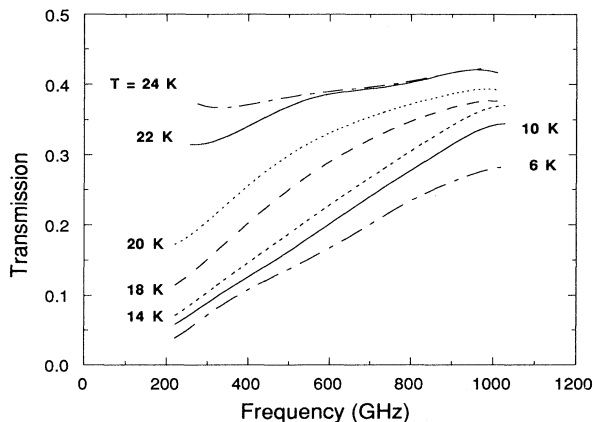


FIG. 2. Frequency-dependent transmission of the BKBO-on-MgO sample in the normal and superconducting states. (Transmissions above 24 K are only weakly temperature dependent and thus, for clarity, are not shown in the figure.)

radical change in pulse shape, implying a dramatic phase shift— or, equivalently, a rapid decrease in the real part of the refractive index of the film—in response to the presence of superconducting carriers.

The changes of the transmitted field can be seen more clearly in the frequency-domain transmission by performing a Fourier transform on the time-domain data. The absolute transmission of the BKBO film at temperatures above and below  $T_c$  is shown in Fig. 2. This frequency regime is of particular interest because it is just below the BCS superconducting gap for BKBO [ $2\Delta(0) = 3.5k_B T_c = 1.5$  THz], and hence it provides a picture of low-energy dynamics for the thermally excited quasiparticles. (The differences between the superconducting and normal states in response to the electromagnetic radiation for  $\omega > 2\Delta$  would quickly disappear with increasing frequency.)

The sample in the normal state is quite transparent and the dc conductivity can be estimated from the finite intercept upon extrapolation to zero frequency. As the film is cooled below  $T_c$  ( $\sim 21$  K), the low-frequency transmission abruptly drops and approaches zero as  $\omega \rightarrow 0$ , suggestive of a dominant response of the imaginary part of the conductivity. The overall transmission level falls with decreasing temperature as the density of superconducting carriers (Cooper pairs) increases. It is the coherent motion of these paired electrons that generates a surface supercurrent and strongly screens the external electromagnetic field.

In an ordinary superconducting film, the transmission increases up to a frequency corresponding to the gap energy,  $2\Delta$ , followed by a drop at higher frequencies due to the onset of photon absorption by pair breaking. Glover and Tinkham confirmed such a peak in transmission for lead and tin films.<sup>29</sup> Recently, a similar peak in transmission<sup>15</sup> and a gaplike onset in absorptivity<sup>30</sup> have been reported for BKBO films. This behavior is quite different from high- $T_c$  cuprates, in which identification of the gap is still controversial and has not been unambiguously confirmed in infrared spectroscopy.<sup>31</sup> For example, previous YBCO transmission measurements<sup>20,21</sup> did not show any gap feature for  $\omega < 350 \text{ cm}^{-1} = 10.5$  THz  $= 5.6k_B T_c$ , nor did measurements in  $\text{Bi}_2\text{Sr}_2\text{CaCu}_2\text{O}_8$  up to  $\omega \leq 650 \text{ cm}^{-1} = 11k_B T_c$ .<sup>32</sup> Although Romero *et al.*<sup>33</sup> did observe a transmission peak in  $\text{Bi}_2\text{Sr}_2\text{CaCu}_2\text{O}_8$  at  $12k_B T_c$  ( $700 \text{ cm}^{-1}$ ), a value far above the predicted BCS gap energy, the feature was interpreted as a consequence either of a midinfrared absorption together with a collapse in the Drude component or of  $4\Delta$  excitations. On the other hand, there are papers, particularly from the early infrared reflectance studies,<sup>34–36</sup> which suggest that an infrared, gaplike feature is observed in cuprates. This feature is manifested by an absorption edge in the reflectance, although its temperature dependence is certainly non-BCS-like in contrast to BKBO. Whether this feature can be tied with an energy gap or a midinfrared absorption is an issue which has generated much controversy. One major difference is that cuprates are in the clean limit (the coherence length is much shorter than the mean-free path,  $\xi \ll l$ , which could make the gap structure difficult to observe),

whereas bismuthates are dirty-limit superconductors. We were, however, unable to identify unambiguously a peak in the transmission data for our BKBO film because the expected BCS gap frequency ( $\sim 1.5$  THz) was above the limit where a poor signal-to-noise ratio existed in our spectra. Although we did see a weak plateau near 1.5 THz (not shown), the large error bars in our data around that frequency prevented us from determining conclusively whether a gap was present or not based directly on the transmission spectra. Alternatively, we will discuss an indirect measurement of the gap after presenting the  $\sigma_2$  data below.

The phase of the transmitted broadband signal through BKBO at different temperatures with respect to the phase in the normal state at 30 K is shown versus frequency in Fig. 3. Above  $T_c$ , like the amplitude of the transmitted signal, the phase has only weak dependence on frequency and temperature. However, in the superconducting state, it exhibits a rapid, negative phase shift and extrapolates to a limit of  $-90^\circ$  at zero frequency for temperatures below 17 K. A near  $-90^\circ$  phase shift implies that the inductive current is dominant over the conduction current, namely,  $\sigma_2 \gg \sigma_1$ , as illustrated next.

Figure 4 plots the imaginary part of the conductivity,  $\sigma_2$ , obtained from the complex transmission by inverting Eq. (1). This quantity characterizes the supercurrent or the nondissipative response of the superconducting electrons. The  $\sigma_2$  in Fig. 4 shows a BCS-like  $1/\omega$  dependence in the superconducting state as predicted by the local theory of electromagnetic response for  $\omega\tau \ll 1$ ,

$$\sigma_2 = \frac{c^2}{4\pi\lambda^2\omega} \propto \frac{f_s}{\omega}, \quad (2)$$

where  $\lambda$  is the magnetic penetration depth and  $f_s$  is the fraction of superconducting carriers.

The  $\sigma_2$  drops quickly with rising  $T$  as the Cooper pairs are rapidly disassociated and are thermally excited across the superconducting gap. Above  $T_c$ , in contrast, the  $1/\omega$

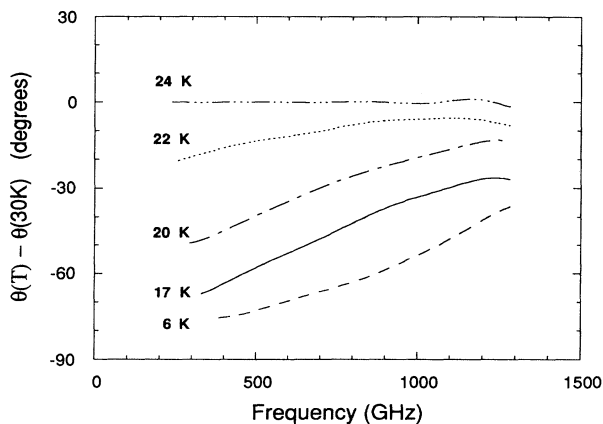


FIG. 3. Frequency-dependent phase shift of the transmitted field through a BKBO film relative to the phase at 30 K. Below  $T_c$ , one observes a dramatic phase change as a result of the rapid condensation of the Cooper pairs.

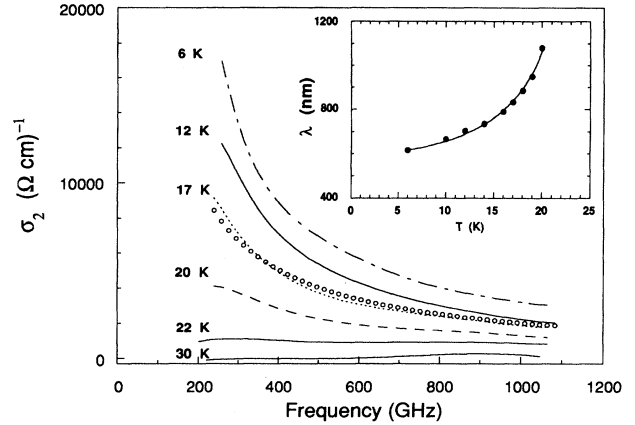


FIG. 4. Imaginary conductivity at temperatures below and above  $T_c$ . A typical  $1/\omega$  fit is represented by open circles for a selected temperature (17 K). Inset: Magnetic penetration depth, with solid dots being data and the solid line being a power-law fit as described in the text.

behavior disappears and  $\sigma_2$  falls to a small level, exhibiting a Drude-like behavior for normal electron response.

The temperature dependence of the magnetic penetration depth in the superconducting state obtained from  $\sigma_2$  using Eq. (2) is shown in the inset of Fig. 4 (solid dots). It does not follow the Gorter-Casimir expression  $\lambda = \lambda(0)/\sqrt{1 - (T/T_c)^4}$ —where  $\lambda(0)$  is the penetration depth at  $T=0$ —nor an exponential  $T$  dependence. Instead, it follows quite well the  $\lambda = \lambda(0)/\sqrt{1 - (T/T_c)^2}$  empirical formula, shown in the inset as a solid line. This functional formula resembles the behavior observed in many YBCO films. Uncertainties in the absolute values of our experimental  $\lambda$  result in part from the uncertainty in film thickness. Because the transmission is governed by the complex surface admittance  $Y = d\sigma$ , an error in  $d$  gives equal errors in  $\sigma_1$  and  $\sigma_2$ , and consequently an error of a constant scaling factor in  $\lambda$ . Nevertheless, this constant factor does not alter the temperature dependence of our  $\lambda$  data. Note that as  $T$  approaches  $T_c$ , larger error bars may exist in the extracted  $\lambda$  because of the growing influence by the thermally excited normal carriers.

The penetration depth of BKBO is larger than that of YBCO for two reasons. First, BKBO has lower carrier concentration, which means a lower conductivity and thus a longer penetration depth compared with YBCO. The other important factor that may increase the  $\lambda$  in BKBO is a large absorption across the gap. In an intermediate or dirty-limit superconductor like BKBO, the quasiparticle relaxation rate  $1/\tau$  is comparable to or larger than the gap  $2\Delta$ . As a result, a large portion of the spectral weight is removed from the  $\delta$  function in  $\sigma_1$  and put into the gap transition. This spectral-weight transfer reduces  $\sigma_2$  or equivalently the number of superconducting electrons, thus significantly increasing the penetration depth.

The  $\lambda$  value obtained here agrees well with that [ $\lambda(0) \approx 550$  nm] reported by Dunmore *et al.*<sup>15</sup> for com-

parable film thicknesses (120–140 nm) using far-infrared techniques in a similar frequency regime, but is greater than the value [ $\lambda(0) \approx 330$  nm] of Pambianchi *et al.*<sup>10</sup> for a much thicker film (360 nm) at 6 GHz using the parallel-plate-resonator (PPR) microwave technique. Note that in both experiments cited above, the absolute values of  $\lambda$  were not measured directly but were instead obtained by model fits to presumed temperature dependencies in  $\lambda$ , whereas the  $\lambda$  reported in this work was derived directly from the experimental data without any assumption about its temperature dependence. Dunmore *et al.*<sup>15</sup> attributed the discrepancy in  $\lambda$  between their values and that of Ref. 10 to a greater electronic scattering in thinner films. It is perhaps also due to a frequency dependence in  $\lambda$ . One should be aware that the microwave field in the PPR experiment could see the substrate dielectric so that resonant frequency and the extracted values of  $\lambda$  would be affected by the substrate if the film thickness is not larger than the penetration depth, as is the case in Ref. 10.

Using our measured values for  $\sigma_2$ , we may also derive information about the temperature dependence of the superconducting gap in BKBO. Tinkham<sup>37</sup> has argued that, in the low-frequency limit ( $\omega \ll 2\Delta$ ),  $\sigma_2$  is related to the BCS gap by

$$\frac{\sigma_2}{\sigma_n} = \frac{\pi\Delta}{\omega} \tanh \frac{\Delta}{2k_B T}, \quad (3)$$

where  $\sigma_n$  is the normal-state real conductivity just above  $T_c$ . This expression is valid in a dirty limit,  $l < \xi$ , which is the case for bismuthates. In order to compare our determination with previous measurements of the energy gap,<sup>7–11,14,15,30</sup> we fit the frequency-dependent  $\sigma_2$  using Eq. (3) to extract  $\Delta(T)$ , shown in Fig. 5. We find that it does follow reasonably well the BCS-like temperature dependence with  $2\Delta(0) = 6.9 \pm 0.4$  meV =  $3.8 \pm 0.2 k_B T_c$ . This result is comparable to that obtained by recent tunneling<sup>8,9</sup> and infrared<sup>14,15,30</sup> measurements, and supports the assignment of the BKBO materials as moderately

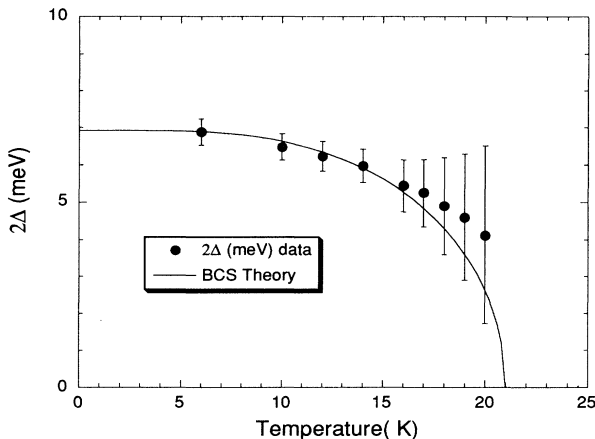


FIG. 5. Temperature dependence of the superconducting gap for BKBO extracted from  $\sigma_2$ . Experimental data (solid dots) are compared with the BCS calculation (solid line).

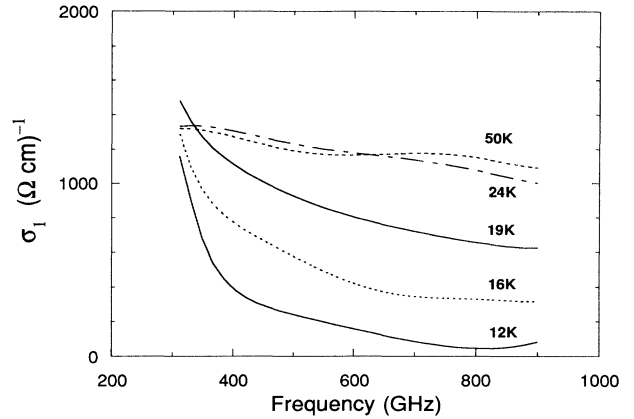


FIG. 6. Real part of the conductivity for the BKBO film at temperatures below and above  $T_c$ . The upturn in the low-frequency  $\sigma_1$  is attributed to coherence effects.

coupled BCS-like superconductors. Errors in  $\Delta(T)$  become increasingly larger at higher temperatures as Eq. (3) is no longer valid for  $T$  near  $T_c$  in the frequency regime presented here because the condition  $2\Delta \gg \omega$  is no longer satisfied. Note that the uncertainty in film thickness does not affect our estimate of the gap values because  $\Delta(T)$  depends only on the normalized  $\sigma_2$  as expressed in Eq. (3).

The real (absorptive) part of the terahertz conductivity is illustrated in Fig. 6. We find that the normal-state  $\sigma_1$  gradually rises as  $T$  is lowered from room temperature (now shown), then has almost no change between 50 K and just above  $T_c$ , implying little temperature dependence in the free-carrier scattering rate. Due to the limited frequency-range data available, fitting the normal-state  $\sigma_1(\omega)$  with a Drude model to find the conductivity width ( $1/\tau$ ) may result in a large error. As an alternative, by extrapolating  $\sigma_1(\omega)$  to zero frequency, one can estimate  $\tau$  from  $\sigma_1(\omega \rightarrow 0) = \omega_p^2 \tau / 4\pi$ . Taking the plasma frequency  $\omega_p = 5300$   $\text{cm}^{-1}$  from Ref. 14 at  $T = 60$  K, we obtain  $1/\tau = 344$   $\text{cm}^{-1} = 43$  meV, which is much greater than  $2\Delta$ ; thus the dirty limit is justified.

Upon entering into the superconducting state, two noteworthy features can be seen. First, the high-frequency  $\sigma_1$  falls rapidly to a regime well below the normal-state value. This resulting “missing-area” effect is expected as the free carriers responsible for the normal-state transport rapidly condense into pairs. The spectral weight under the  $\sigma_1(\omega)$  curve is removed from the finite frequencies and shifted to the  $\delta$  function  $\delta(\omega)$  to form a superconducting condensate. Second,  $\sigma_1$  rises quickly as frequency is decreased below 500 GHz and exhibits a divergent  $\omega$  dependence toward zero frequency. The conductivity tends to pass the normal-state value at our low-frequency limit. However, it does not show a maximum at any temperature below  $T_c$  throughout the frequency range measured. This is in contrast to the well-known results of high- $T_c$  cuprates, in which a well-defined peak in  $\sigma_1(T)$  has been reported at microwave,<sup>38,39</sup> terahertz,<sup>22</sup> and far-infrared<sup>40</sup> frequencies. Such a peak in HTS’s has been attributed to a rapid col-

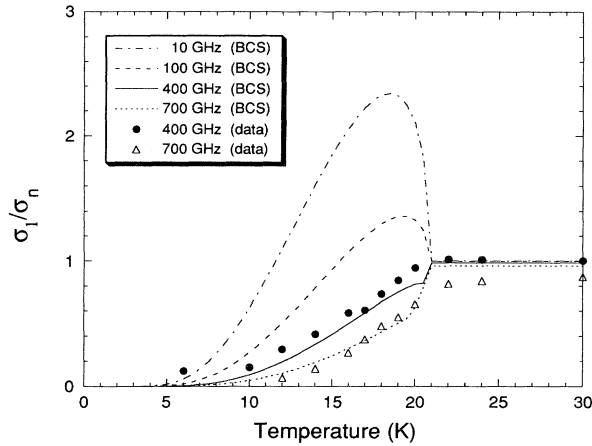


FIG. 7. Temperature-dependent experimental conductivity for BKBO film (solid dots and open triangles) normalized to the normal-state dc conductivity at two selected frequencies in comparison to calculations (curves) based on the intermediate-limit BCS theory using parameters of  $2\Delta=7$  meV=1.7 THz,  $l/\pi\xi=0.25$ , and  $T_c=21$  K.

lapse in the quasiparticle scattering rate.

The lack of a maximum in  $\sigma_1$  also appears to be contrary to the prediction of a peak in  $\sigma_1(T)$  due to the BCS case-II coherence factors. It must, however, be pointed out that such a BCS coherence peak should only occur at frequencies much below the gap energy of the material. In dirty-limit BCS superconductors, for  $\omega > T_c/2$  (or  $\omega/2\Delta > 15\%$ ), where the photon energy is larger than the width of the singular density of states near the gap edge, the  $\sigma_1(T)$  no longer shows a peak.<sup>41</sup> For our film, the gap  $2\Delta(0)\approx 7$  meV=1.7 THz, and thus the coherence peak would occur only below 250 GHz, a regime essentially beyond our detection limit. To investigate the behavior of  $\sigma_1$  in more detail, we plot it as a function of temperature at two selected frequencies, shown in Fig. 7. The experimental data exhibit a monotonic dependence on temperature below  $T_c$ . As demonstrated in Fig. 7, our results are in fact in remarkable agreement with the theoretical curves calculated in the framework of BCS theory using the Chang-Scalapino formula,<sup>42</sup> a generalization of the Leplae<sup>43</sup> equation in the intermediate limit. At  $T \ll T_c$ , the theory predicts an exponential decay in  $\sigma_1$  with falling temperature because of the vanishing density of states. A peak would develop only at microwave frequencies as illustrated in Fig. 7 for 100 and 10 GHz in the BCS calculation. Indeed, such a tendency of a peak is manifested in our experimental data (Fig. 6) by a rapid

low-frequency upturn in  $\sigma_1$ . Therefore, we attribute this upturn to the BCS coherence effects.

#### IV. CONCLUSIONS

In conclusion, we have explored the superconducting properties of a  $\text{Ba}_{1-x}\text{K}_x\text{BiO}_3$  film by measuring its millimeter- and submillimeter-wave complex transmission over a frequency range which until now has not been investigated. As the sample enters into superconducting transition, a strong pulse reshaping in the time-domain spectra and a dramatic decrease in both the magnitude and phase of the transmitted electric field in the frequency-domain spectra are observed. A strong  $1/\omega$  dependence is seen in the imaginary conductivity from which a BCS-like gap  $2\Delta(0)=6.9$  meV is inferred. Our data compare well with the temperature dependence of an isotropic *s*-wave-like BCS gap. The penetration depth extracted directly from the complex transmission gives  $\lambda(0)=6000$  Å. The conductivity and the penetration depth values suggest that the film is in an intermediate or dirty limit, as distinguished from the extremely clean-limit high- $T_c$  cuprates. Also, unlike cuprates, in which the quasiparticle scattering rate,  $1/\tau$ , is linearly temperature dependent with a zero intercept in the normal state and collapses rapidly below  $T_c$  to give a peak in  $\sigma_1(T)$  at low frequencies, the bismuthates have an essentially temperature-independent scattering rate. No  $\sigma_1(T)$  peak is observed in the frequency range measured and our data exhibit a trend suggesting a peak due to BCS coherence effects may occur for frequencies below 250 GHz. Given the characteristics stated above together with the existing studies in the infrared and microwave regimes,<sup>10,11,14,15,30</sup> a consistent picture emerges which suggests that BKBO materials are moderately coupled BCS-like intermediate- or dirty-limit superconductors. Finally, our experimental technique can also be extended to study the superfluid response of high- $T_c$  materials to optical radiation by illuminating such films with a synchronized laser beam. Studies on BKBO and YBCO will be presented in future publications and may shed further light on the issue of bolometric or nonbolometric response of high- $T_c$  superconductors.

#### ACKNOWLEDGMENTS

Work at the University of Michigan was supported by the National Science Foundation through the Center for Ultrafast Optical Science under Contract No. STC PHY 8920108. At the University of Illinois, the work was supported under Grant No. NSF-DMR-91-20000 through the Science and Technology Center for Superconductivity.

\*Present address: Department of Physics and Science and Technology Center for Superconductivity, University of Illinois at Urbana-Champaign, Urbana, Illinois 61801.

†Also with Department of Physics, University of Michigan, Ann Arbor, Michigan 48109.

‡Also with Department of Physics and Materials Research Laboratory, University of Illinois at Urbana-Champaign, Urbana, Illinois 61801.

<sup>1</sup>A. Fathy, D. Kalokitis, and E. Belohoubek, *Microwave J.* **31**(10), 75 (1988).

- <sup>2</sup>S. M. Anlage, M. S. Pambianchi, A. T. Findikoglu, C. Dougherty, D. Wu, J. Mao, S. Mao, X. X. Xi, T. Vankatesan, J. L. Peng, and R. L. Greene, in *Oxide Superconductor Physics and Nano-Engineering*, edited by D. Pavuna [Proc. SPIE **2158**, (1994)].
- <sup>3</sup>B. Batlogg, R. J. Cava, L. W. Rupp, Jr., A. M. Muzsice, J. J. Krajewski, J. P. Remeika, W. F. Peck, Jr., A. S. Copper, and G. P. Espinosa, Phys. Rev. Lett. **61**, 1670 (1988).
- <sup>4</sup>H. Sato, H. Takagi, and S. Uchida, Physica C **169**, 391 (1990).
- <sup>5</sup>Q. Huang, J. F. Zasadzinski, N. Tralshawala, K. E. Gray, D. G. Hinks, J. L. Peng, and R. L. Greene, Nature (London) **347**, 369 (1990); Q. Huang, J. F. Zasadzinski, K. E. Gray, D. R. Richards, and D. G. Hinks, Appl. Phys. Lett. **57**, 2356 (1990).
- <sup>6</sup>A. N. Pargellis, F. Sharifi, R. C. Dynes, B. Miller, E. S. Hellman, J. M. Rosamilia, and E. H. Hartford, Appl. Phys. Lett. **58**, 95 (1991).
- <sup>7</sup>B. M. Moon, C. E. Platt, R. A. Schweinforth, and D. J. Van Harlingen, Appl. Phys. Lett. **59**, 1905 (1991).
- <sup>8</sup>A. Kussmaul, E. S. Hellman, E. H. Hartford, and P. M. Tedrow, Appl. Phys. Lett. **63**, 2824 (1993).
- <sup>9</sup>H. Sato, T. Ido, S. Uchida, S. Tajima, M. Yoshida, K. Tanabe, K. Tatsuahara, and N. Miura, Phys. Rev. B **48**, 6617 (1993).
- <sup>10</sup>M. S. Pambianchi, S. M. Anlage, E. S. Hellman, E. H. Hartford, Jr., M. Bruns, and S. Y. Lee, Appl. Phys. Lett. **64**, 244 (1994).
- <sup>11</sup>Z. Schlesinger, R. T. Collins, A. Calise, D. J. Hinks, A. W. Mitchell, Y. Zheng, B. Dabrowski, N. E. Bickers, and D. J. Scalapino, Phys. Rev. B **40**, 6862 (1989).
- <sup>12</sup>S. H. Blanton, R. T. Collins, K. H. Kelleher, L. D. Rotter, Z. Schlesinger, D. G. Hinks, and Y. Zheng, Phys. Rev. B **47**, 996 (1993).
- <sup>13</sup>M. A. Karlow, S. L. Cooper, A. L. Kotz, M. V. Klein, P. D. Han, and A. Payne, Phys. Rev. B **48**, 6499 (1993).
- <sup>14</sup>A. V. Puchkov, T. Timusk, W. D. Moseley, and R. N. Shelton, Phys. Rev. B **50**, 4144 (1994).
- <sup>15</sup>F. J. Dunmore, H. D. Drew, E. J. Nicol, E. S. Hellman, and E. H. Hartford, Phys. Rev. B **50**, 643 (1994).
- <sup>16</sup>Frederick Wooten, *Optical Properties of Solids* (Academic, New York, 1972).
- <sup>17</sup>J. Orenstein, G. A. Thomas, A. J. Millis, S. L. Cooper, D. H. Rapkine, T. Timusk, L. F. Schneemeyer, and J. V. Waszczak, Phys. Rev. B **42**, 6342 (1990).
- <sup>18</sup>K. Kamaras, S. L. Herr, C. D. Porter, N. Tache, D. B. Tanner, S. Etemad, T. Venkatesan, E. Chase, A. Inam, X. D. Wu, M. S. Hegde, and B. Dutta, Phys. Rev. Lett. **64**, 84 (1990).
- <sup>19</sup>F. Gao, D. B. Romero, D. B. Tanner, J. Talvacchio, and M. G. Forrester, Phys. Rev. B **47**, 1036 (1993).
- <sup>20</sup>F. Gao, G. L. Carr, C. D. Porter, D. B. Tanner, S. Etemad, T. Vankatesan, A. Inam, B. Dutta, X. D. Wu, G. P. Williams, and C. J. Hirschmugl, Phys. Rev. B **43**, 10383 (1991).
- <sup>21</sup>S. Cunsolo, P. Dore, S. Lupi, R. Trippetti, C. P. Varsamis, and A. Sherman, Physica C **211**, 22 (1993).
- <sup>22</sup>M. C. Nuss, P. M. Mankiewich, M. L. O'Malley, E. H. Westerwick, and P. B. Littlewood, Phys. Rev. Lett. **66**, 3305 (1991).
- <sup>23</sup>J. F. Whitaker, F. Gao, and Y. Liu, in *Nonlinear Optics for High-Speed Electronics and Optical Frequency Conversion*, edited by N. Peygambarian, H. Everitt, R. C. Eckardt, and D. D. Lowenthal [Proc. SPIE **2145**, 168 (1994)].
- <sup>24</sup>M. van Exter and D. R. Grischkowsky, IEEE Trans. Microwave Theory Tech. **38**, 1684 (1990).
- <sup>25</sup>S. Gupta, M. Y. Frankel, J. A. Valdmanis, J. F. Whitaker, G. A. Mourou, F. W. Smith, and A. R. Calawa, Appl. Phys. Lett. **59**, 3276 (1991).
- <sup>26</sup>C. E. Platt, R. A. Schweinforth, M. R. Teepe, and D. J. van Harlingen, in *Lattice Effects of High- $T_c$  Superconductors Conference*, edited by Y. Bar-Yan (World Scientific, Singapore, 1991).
- <sup>27</sup>D. J. Hinks, A. W. Mitchell, Y. Zheng, D. R. Richards, and B. Dabrowsky, Appl. Phys. Lett. **54**, 1585 (1989).
- <sup>28</sup>D. Grischkowsky and S. Keiding, Appl. Phys. Lett. **57**, 1055 (1990).
- <sup>29</sup>R. E. Glover and M. Tinkham, Phys. Rev. **108**, 243 (1957).
- <sup>30</sup>D. Miller, P. L. Richards, E. J. Nicol, E. S. Hellman, E. H. Hartford, C. E. Platt, R. A. Schweinforth, D. J. Van Harlingen, and J. Amano, J. Phys. Chem. Solids **54**, 1323 (1994).
- <sup>31</sup>For a review, see D. B. Tanner and T. Timusk, in *Physical Properties of High Temperature Superconductors III*, edited by D. M. Ginsberg (World Scientific, Singapore, 1992), p. 363.
- <sup>32</sup>D. Mandrus, M. C. Martin, C. Kendziora, D. Koller, L. L. Forro, and L. Mihaly, Phys. Rev. Lett. **70**, 2629 (1993).
- <sup>33</sup>D. B. Romero, G. L. Carr, D. B. Tanner, L. Forro, D. Mandrus, L. Mihaly, and G. P. Williams, Phys. Rev. B **44**, 2818 (1991).
- <sup>34</sup>G. A. Thomas, J. Orenstein, D. H. Rapkine, M. Capizzi, A. J. Millis, R. N. Bhatt, L. F. Schneemeyer, and J. V. Waszczak, Phys. Rev. Lett. **61**, 1313 (1988).
- <sup>35</sup>J. Schutzmann, W. Ose, J. Keller, K. F. Renk, B. Roas, L. Schultz, and G. Saemann-Ischenko, Europhys. Lett. **8**, 679 (1989).
- <sup>36</sup>Z. Schlesinger, R. T. Collins, F. Holtzberg, C. Feild, S. H. Blanton, U. Welp, G. W. Crabtree, Y. Fang, and J. Z. Liu, Phys. Rev. Lett. **65**, 801 (1990).
- <sup>37</sup>M. Tinkham, *Introduction to Superconductivity* (McGraw-Hill, New York, 1975).
- <sup>38</sup>D. A. Bonn, R. Liang, T. M. Riseman, D. J. Baar, D. C. Morgan, K. Zhang, P. Dosanjh, T. L. Duty, A. MacFarlane, G. D. Morris, J. H. Brewer, W. N. Hardy, C. Kallin, and A. J. Berlinsky, Phys. Rev. B **47**, 11314 (1993).
- <sup>39</sup>F. Gao, J. W. Kruse, C. E. Platt, M. Feng, and M. V. Klein, Appl. Phys. Lett. **63**, 2274 (1993).
- <sup>40</sup>D. B. Romero, C. D. Porter, D. B. Tanner, L. Forro, D. Mandrus, L. Mihaly, G. L. Carr, and G. P. Williams, Phys. Rev. Lett. **68**, 1590 (1992).
- <sup>41</sup>J. R. Schrieffer, *Theory of Superconductivity* (Benjamin, New York, 1964).
- <sup>42</sup>J. Chang and D. J. Scalapino, Phys. Rev. B **40**, 4299 (1989).
- <sup>43</sup>L. Leplae, Phys. Rev. B **27**, 1911 (1983).